



DENSELY CROSS-LINKED POLYSILOXANE NANOGELS

Cite this: *INEOS OPEN*,
2020, 3 (4), 118–132
DOI: 10.32931/io2022r

Received 7 August 2020,
Accepted 25 August 2020

<http://ineosopen.org>

I. B. Meshkov,*^a A. A. Kalinina,^a V. V. Kazakova,^a and A. I. Demchenko^b

^a *Enikolopov Institute of Synthetic Polymeric Materials, Russian Academy of Sciences,
ul. Profsoyuznaya 70, Moscow, 117393 Russia*

^b *Nesmeyanov Institute of Organoelement Compounds, Russian Academy of Sciences,
ul. Vavilova 28, Moscow, 119991 Russia*

Abstract

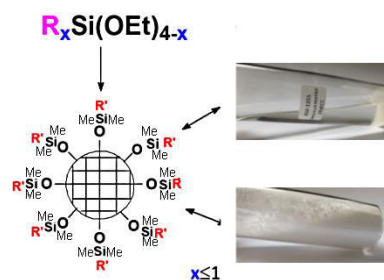
Nanogels can be called the new old[§] objects of polymer chemistry. New because we have formulated the criteria for the assignment of objects to this group within the macromolecule-particle concept and developed the methods for their directed and controlled synthesis. Old because the application of these criteria to the earlier known systems allows us to surely classify them as nanogels. It is shown that this classification *per se* provides insight into the organization of their molecular structures and enables directed modification. This means a transition from the empirical control of the properties to molecular design. The current review presents a brief historical overview of densely cross-linked nanogels and their main synthetic routes and highlights the principles and approaches to the control of their structures and molecular-mass characteristics, application scope, and prospects for further development.

Key words: nanogels, densely cross-linked polysiloxanes, molecular silica sols, MQ copolymers, hyperbranched polysiloxanes.

Introduction

The term "nanogels" is used in the scientific literature for a long time to define the cross-linked polymer systems featuring nanoscale sizes. Its appearance is stipulated by the development of concepts about microgels, which have smaller dimensions [1–6]. In this review, we use the term "densely cross-linked nanogels" since these objects strongly differ from simple nanogels, which structures are almost not defined. Densely cross-linked nanogels are polycyclic spatial network structures which sizes are artificially restricted by different methods: either high dilution in a gas phase or the medium of an organic solvent or by addition of a special agent that terminates the particle growth. It would be more logical to use the term "nanonetworks", but since the time of polymer classics who used the conventional term of gel formation instead of the dissonant term of network formation [7], all researchers stick to the same choice. Let us also adhere to this tradition.

The definition "densely cross-linked" is principal for nanogels as well as the prefix "hyper" in hyperbranched polymers, which emphasizes their qualitative difference from simply branched polymers, or the word "dense" before molecular brushes or multi-star polymers compared to simple star-shaped polymers. All these additions stem from the impossibility to fit these specific objects to a general classification of polymers by the chain structure and the necessity to attribute them to a separate group of



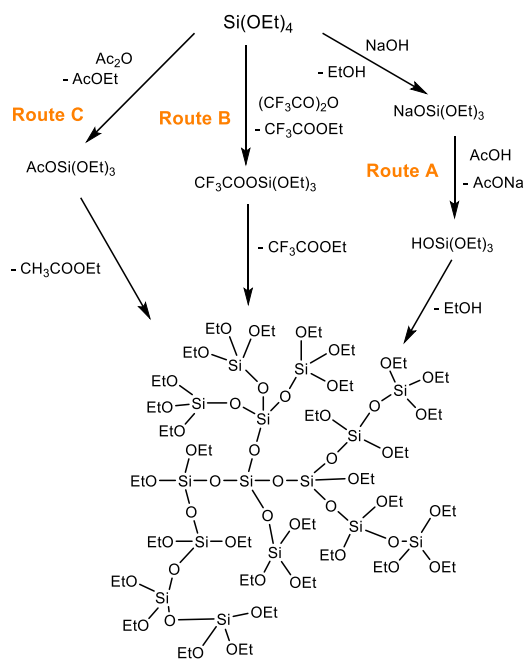
macromolecule-particles or, in other coordinates, macromolecular nanoobjects [8–10]. The necessity to separate these objects into a special group was suggested for the first time by D. Tomalia and P. Dvornic but they motivated this suggestion for some other reasons [11].

Hence, we attributed densely cross-linked nanogels (DCNGs) to macromolecular nanoobjects that have a double nature of macromolecules and particles. What is the basis for this classification? What are the criteria for this? Which properties are characteristic of these molecular systems? To answer these and other questions, we should follow the historical background of these objects and methods for their production and structure identification and consider the existing analogs. If we add to this the investigation of their potential practical application, the answers to these questions will comprise the goal of this short review.

Molecular silica sols

Molecular silica sols (MSs) were historically the first polysiloxane DCNGs that were synthesized in a directed manner. A convenient precursor for their production appeared to be hyperbranched polyethoxysiloxane (HBPEOS) which can be obtained by three methods (Scheme 1) [12–14].

The main idea of route A consists in the generation of sodium oxytriethoxysilane according to the published procedure [14] followed by its neutralization with acetic acid and polycon-



Scheme 1. Synthetic routes to HBPEOS.

densation of the resulting silanol. The synthesis conditions were chosen to promote the polymer formation predominantly by the second direction of two possible mechanisms of silanol condensation: homofunctional mechanism with water release and heterofunctional mechanism with alcohol release. In this case, the synthetic route meets the requirements for the formation of a hyperbranched structure. For this purpose, the process was carried out by slow addition of dilute acetic acid to a solution of the sodium salt. The ethoxy groups in sodium alkoxysilanes appeared to be activated compared to the hydroxy-substituted reagents. The chosen order of addition of the reagents provided a heterofunctional character of the process: the hydroxy groups resulting from neutralization were in a predominant excess of the ethoxy groups. Triethylamine, known as a catalyst of the heterofunctional condensation of hydroxy and ethoxy groups during the formation of a silicate structure, was added to the reaction mixture prior to the salt.

The second scheme (route B) includes the interaction of tetraethoxysilane with trifluoroacetic anhydride with intermediate formation of triethoxy(trifluoroacetoxy)silane followed by heterofunctional condensation of this compound. The attractive feature of this method is the homogeneous character of the whole process, from the mixing of the reagents to the production of resulting ethyl silicate.

The third synthetic approach to HBPEOS [15] is based on the polycondensation of tetraethoxysilane with acetic anhydride in the presence of an organotin catalyst (route C). According to the results of partition chromatography and viscosity studies, the average molar mass and molar mass distribution of the products obtained by this method increased exponentially as the molar ratio of acetic anhydride to tetraethoxysilane increased from 1.0 to 1.2. At the molar ratio of 1.3, a solid gel was formed.

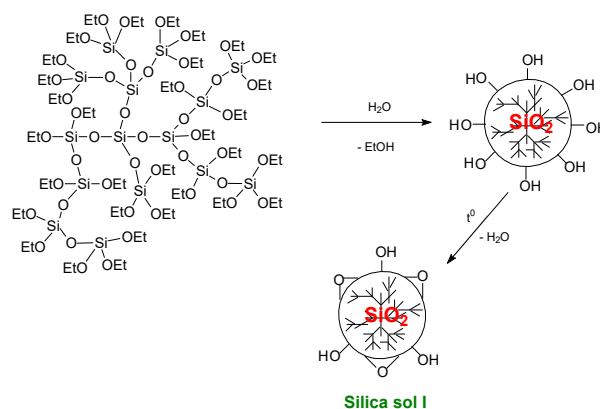
The functional MSs were obtained by the hydrolysis of HBPEOS in dilute solutions of polar solvents followed by its intramolecular cyclization [16] (Scheme 2).

The resulting polymers were fully soluble and their solutions featured low viscosities. This implies that a macronetwork was

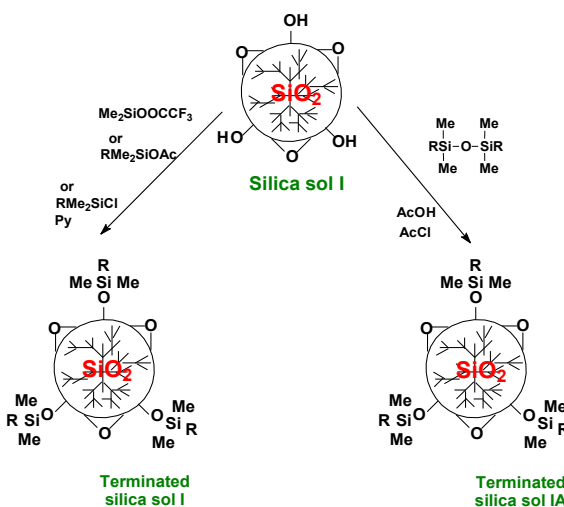
not formed; instead, the silicon dioxide sols stable in dilute solutions were obtained. Taking into account the high initial functionalization degree of the system and the conversion of functional groups, the only one alternative to the formation of a macronetwork was polycyclization; the retention of solubility was defined by solvation of residual functional groups. This means that MS is a metastable state of silicon dioxide, which readily converts to a common stable state—silica gel—during solution concentrating. The fact of isolation of silica sols is trivial and is widely used in practice [17]. A peculiarity of this approach is the stabilization of the form that is soluble in organic solvents. This is nonsense: sand is soluble in an organic medium! On the other hand, the level of concentrations at which these objects retained their solubility and stability reached 20% and more.

To analyze the MS structure, the silanol groups were terminated with trimethylsilyl moieties using trimethyltrifluoroacetoxysilane as a terminating agent (Scheme 3).

Terminated silica sols I were studied by elemental analysis, gel permeation chromatography, and small-angle X-ray scattering (SAXS). It was established that, in dilute solutions, the volume fraction of large particles with $R_g > 20$ nm does not exceed 5%, which evidences the lack of aggregation processes of the resulting silica sols.



Scheme 2. Synthesis of functional MSs from HBPEOS.



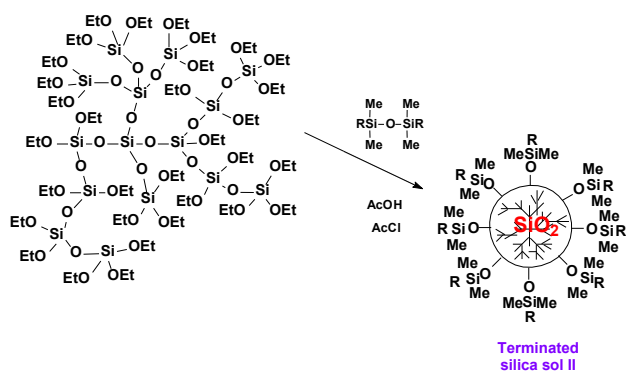
Scheme 3. Synthesis of terminated MSs; R is any organic group (hydride, methyl, vinyl, phenyl, *etc.*).

The nature of solubility of nonterminated MSs is easy to understand: it depends on the concentration of hydroxy groups that are solvated by THF or other polar solvents. After the removal of a solvating solvent or its substitution for a nonsolvating one (hexane, toluene), the silica sol immediately converted to a silica gel (irreversibly). At the same time, MSs are rather stable in the solvated state and can be stored in dilute solutions at room temperature without apparent changes for years. According to the results of the functional and elemental analyses, the silica sol corresponds to the empirical formula $(\text{Si}_2\text{O}_{3.5}\text{OH})_n$, 90% of the involved hydroxy groups are available for substitution. The MSs applied from solution on the mica surface were studied by atomic force microscopy. The micrographs clearly show the spherical objects adsorbed on the mica surface. According to the AFM data, the particle sizes of the adsorbed silica sol range from 6 to 10 nm, which is in good agreement with the results of the SAXS experiments, if take into account that drying is accompanied by the formation of secondary aggregates on the surface.

The results of chemical transformations explored by different methods suggest that the silica sols represent silica particles which possess individual molecular structures, unlike most of the known amorphous silicas which represent supramolecular structures—large aggregates. The stabilization of MSs in solutions became possible owing to the fact that among different processes, which take part in their synthesis, two main processes, namely, the formation of intermolecular contacts and intramolecular cyclization, can be identified and separated in space and time. Such a separation will be considered below by several examples.

Our research group used three methods for the synthesis of nonfunctionalized terminated silica sols. The first method consisted in the preliminary synthesis of polyhydroxy-functionalized silica sol (silica sol I) from HBPEOS (Scheme 2) followed by modification of a shell with trimethylsilyl groups using trimethylchlorosilane in the presence of an acceptor (terminated silica sol I) (Scheme 3).

The second method for the synthesis of nonfunctionalized silica sols (Scheme 4) was based on the polycondensation of HBPEOS in an active medium with concomitant termination of the alkoxy groups with hexamethyldisiloxane in the presence of acetyl chloride as a catalyst, which served as a source of anhydrous HCl.



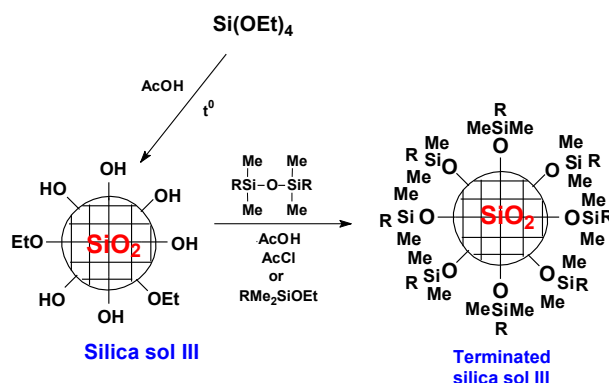
Scheme 4. Synthesis of terminated MSs from HBPEOS by the condensation in an active medium (method 2). R is any organic group (hydride, methyl, vinyl, phenyl, *etc.*).

Using hexamethyldisiloxane and dry HCl in acetic acid, silica sol I was terminated by the same method to afford terminated silica sol IA (Scheme 3). However, during the formation of nonfunctionalized nanogels in an active medium, the process of termination and intermolecular interactions between primary structures proceeded simultaneously, which facilitated the formation of larger particles (terminated silica sol IA, terminated silica sol II) unlike terminated silica sol I, for which the formation of molecular structures was almost deprived of the interaction of primary silica sols with each other (Scheme 3).

Hence, the first two methods for the synthesis of nonfunctionalized nanogels are based on the application of the same precursor, namely, HBPEOS. These methods encompass a sequence of transformations of the hyperbranched structure and its combination with the termination reaction and provoke the formation of a nonregular structure with the nonordered arrangement of siloxane units in the resulting structure.

The third approach to nonfunctional silica sols (Scheme 5) implies the alternative formation of a siloxane core from a monomer—tetraethoxysilane. The formation of the silica core (silica sol III) proceeds under conditions of an active medium—during a cascade process of hydrolytic polycondensation [19]. In all cases, the primary objects are converted to a nonfunctional state by termination. A distinctive feature of the termination process is the fact that it means the termination of aggregation of silica particles owing to the formation of a nonfunctional inert shell. The completeness of condensation and termination was controlled by ^1H NMR and IR spectroscopies. The high efficiency of termination provides the resulting silica sols with stability and allows one to study them both in bulk and solutions of different solvents. It is noteworthy that, independent from the method for production of the above-mentioned nonfunctional systems, all the particles obtained had the same chemical composition that corresponds to the formula $[\text{Me}_3\text{SiO}_{0.5}]_x[\text{SiO}_2]_y$.

All the silica sols were thoroughly characterized by a complex of physicochemical methods. Their behavior in solution was studied through the evaluation of the values of characteristic viscosity in different solvents, molar masses, and hydrodynamic radii. Furthermore, their properties in bulk were analyzed based on the glass-transition points and the structures of the modified silicas from different series explored by means of wide-angle X-ray scattering (WAXS).



Scheme 5. Synthesis of the terminated MSs from tetraethoxysilane (method 3). R is any organic group (hydride, methyl, vinyl, phenyl, *etc.*).

The detailed study of the resulting modifications of molecular nanogels started from fractioning. The GPC chromatograms showed that the silica samples obtained by the above-mentioned methods feature wide molar mass distribution. To gain further insight, the fractioning to narrow-disperse fractions was carried out using preparative GPC. Figure 1 depicts the GPC curves of initial terminated silica sol I and its fractions.

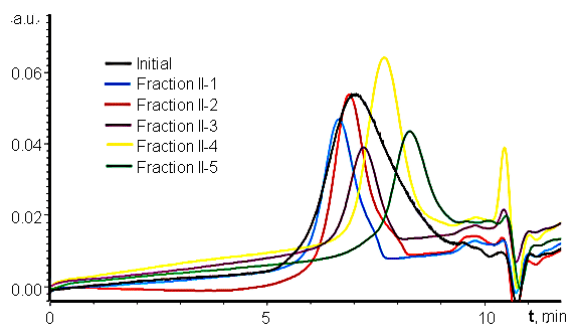


Figure 1. GPC curves of terminated silica sol I and its fractions.

The analysis of characteristic viscosities of the fractions showed that all the samples behave as compact globular particles. The changes in the viscosities of the same fractions in polar and nonpolar solvents remained miserable. The results obtained allowed us to characterize these silica sols as objects that have a double nature. The polymeric nature of the resulting hybrid particles is manifested in a tendency to form molecular solutions in organic solvents. The compact globular shape and minimal response to the changes in solvent nature are associated with the behavior typical for solid impermeable particles.

The dynamic light scattering (DLS) studies showed that the samples feature a very narrow distribution of the hydrodynamic radii, which can be caused by the non-associated globular forms. In the case of methyl *tert*-butyl ether (MTBE) as a solvent, the values of hydrodynamic radii of the fractions were higher than those in toluene at an average of 15%. These data are in good agreement with the results of viscometry studies, where the values of characteristic viscosity were higher in polar MTBE than in toluene.

For comparison, the molar masses and hydrodynamic radii of the resulting fractions of silica particles were also defined using the universal calibration of the GPC data. A gradual change in the size, molar mass, and characteristic viscosity was observed. Quite a broad range of the fractions under consideration (from several to hundreds of thousands a.m.u.) evidences the representativeness of a series of the hybrid nanoparticles. At the qualitative level, the resulting values of molar masses are in good agreement with the analogous data for organosilicon dendrimers featuring comparable sizes [20].

The investigation of thermomechanical curves of the samples obtained (Fig. 2) allowed us to follow a correlation between the growth of the glass-transition point and an increase in the molar mass of the samples, which would have been natural if it was not for the rapid exceeding of T_g over the values above the decomposition points >300 °C. In this case, it seems to be more logical to correlate T_g with a core-shell ratio. In all three series of the samples, the glass-transition points exceed the decomposition points as soon as the sizes of the silica core start

to define the properties of the sample. Since it was nonmelting within the considered limits, the strain appeared only with the beginning of the processes of thermal destruction of the trimethylsilyl shell. This means a qualitative transition in the systems inorganic core–organic shell with a change in the core-shell ratio.

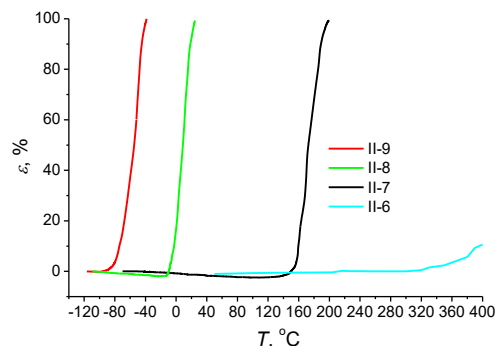


Figure 2. Thermomechanical curves of the fractions of terminated silica sol I.

Based on the results of investigations on the properties of the isolated fractions, a model for the transition of a macromolecule to a particle was suggested. Within this model, a macromolecule features the mobility of separate structural units ($T_g < T_{dec}$) and almost full solvation of a molecular moiety, which is characteristic of polymeric particles. The particle is characterized only by the solvation of a shell and the lack of molecular mobility of the core (in this case, the core represents a rigid dense network: $T_g > T_{dec}$). Subsequently, the use of this model allowed for defining the composite nature of a popular group of materials, namely, MQ resins [21].

Even in the case of the uniformity of the particles obtained by three different methods, their fine molecular structures differ. This becomes evident from the results of the WAXS studies. Thus, the comparison of the structures of silica cores of the samples obtained by the second and third methods suggests that the synthetic route affects the core structure of the resulting particles of modified silicon dioxide. The comparison of silicas obtained by routes 2 and 3 shows that the cores of these particles are ordered but, in the first case, the fraction of the ordered part is substantially lower than that in the second case. The cores of the particles obtained by the first method are fully amorphous. Taking into account the peculiarities of the synthetic routes, these differences seem to be expected. During exclusive intramolecular cyclization, it is very difficult for a hyperbranched structure to form an ordered structure—route 1. The possibility of occurrence of intermolecular reactions along with the intramolecular ones ensures even greater opportunities for ordering—route 2. Finally, the formation of a core from monomer units is a direct route to the most ordered structure—route 3.

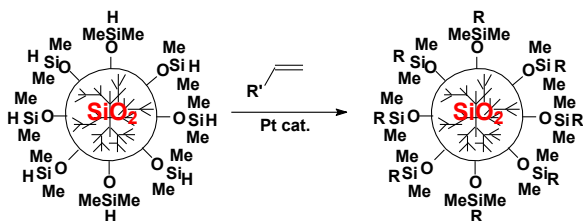
The investigation of the resulting fractions by the Langmuir method [22] at the water–air interface also allowed the detection of the transition from a macromolecule to a particle. Of course, these experiments require further exploration with the more narrow disperse fractions.

Hence, in all the considered cases we have the compounds of almost the same compositions, which are constructed

according to the core-shell principle and represent the so-called DCNGs. The nanogels include the well-known aerosils since they are produced by burning silicon tetrachloride in a hydrogen flame at high dilution and these conditions meet the production of nanodisperse particles that possess all characteristics of DCNGs. Due to harsh synthetic conditions (high temperatures, acid medium), the condensation processes occur much deeper and, therefore, the residual content of the hydroxy groups does not exceed 1.5% before annealing. They are fully amorphous because, due to the powerful energetic background, the advantages of ordered forms over random arrangement level out.

Nevertheless, let us return to silica sols. The termination of silica sols, on the one hand, converts them to stable forms for investigation of the properties and, on the other hand, endows them with some new qualities because it enables the generation of new functional groups on their surfaces that can be utilized in different processes. Furthermore, to use them as fillers for different polymeric matrices, it seems reasonable to use the particle shell close to the matrix. This implies that the termination can transform from an auxiliary operation to the method for adopting silica molecular particles and their molecular parameters to a certain polymeric matrix. Hence, the core is a nanofiller which can strongly differ in the chemical nature from a particular polymeric matrix. The shell minimizes the problem of rejection of a nanoobject by the polymeric matrix that inevitably leads to particle aggregation.

The termination of silica sol with tetramethyldisiloxane (by any method) can afford hydride-functionalized silica sol [23]. The latter, in turn, can be modified with different organic shells to introduce into polymer matrices such as polyepoxides, polyacrylates, polystyrene, and others. Thus, for example, the DCNGs particles were modified by the hydrosilylation with styrene (Scheme 6) to introduce into a polystyrene matrix [24].



Scheme 6. General scheme for the modification of hydride-functionalized silica sols with different compounds bearing double bonds by the hydrosilylation (R is any organic group, for example, decyl, 2-phenylethyl, polar groups with ethylene glycol moieties, etc.).

The modified silica was combined with polystyrene by the introduction of a molecular filler to the polymer melt. (This will be discussed in detail in the section devoted to the application of DCNGs).

To introduce silica sols into polar matrices such as poly(ethylene glycol) or polylactide (PLA), the silica sol particles with polar groups on the periphery were synthesized [25]. The termination with polar methoxymono-, di-, and triethylene glycol groups was accomplished by several approaches. The first one was based on the hydrosilylation of the hydride-functionalized silica sol with an allyl ether of mono-, di- and triethylene glycols bearing methoxy groups at the ends (Scheme 6). The second approach consisted in the termination of polyhydroxy-functionalized silica sol in an active medium

with dimethylacetoxysilane having di- or triethylene glycol substituent (Scheme 3). The third approach was based on the synthesis of silica sols from tetraethoxysilane followed by termination at the final step again with dimethylacetoxysilane bearing di- or triethylene glycol substituent (Scheme 5). Furthermore, the silica sols bearing acetoxymethyltrimethylsilyl groups on the periphery were synthesized by the termination of the polyhydroxy silica sol with the corresponding acetoxy silane (Scheme 3). And the third type of silica sols described in this work is the silica sol with methoxyacetoxymethyltrimethylsilyl terminal units. It was obtained by two methods: the former was based on HBPEOS and included the condensation in an active medium and termination with methoxyacetoxymethyltrimethylsilanol (Scheme 4); the second one started from tetraethoxysilane and included the condensation followed by termination with methoxyacetoxymethyltetramethyldisiloxane (Scheme 5). All the resulting DCNGs were fractionated and characterized by GPC; the resulting fractions were tested for the characteristic viscosity. The viscosity values of almost all the DCNGs indicate that these hybrid systems behave analogously to the model systems thoroughly studied in Ref. [22]. This means that their behavior can be described in terms of the model macromolecule-particle, although the more correct interpretation, especially in the case of the fractionated samples, requires additional detailed thermomechanical studies.

A possibility of the formation of a hydrophilic surface layer was demonstrated in Ref. [26]. The silica sol bearing 3-hydroxypropyl groups in the shell were obtained according to the above-described method based on the hydrosilylation of a functional silica sol with trimethylallyloxysilane (Scheme 6) followed by the removal of the trimethylsilyl protecting groups. According to the results of SAXS analysis, the nanosized particles of the silica sol bearing 3-hydroxypropyl surface groups were well dispersed in methanol; the formation of aggregates was not observed.

The examples of the introduction of these particles with polar groups in the shell into poly(ethylene oxide) [27] or polylactide [28] matrices will be considered further in the section devoted to the application of DCNGs.

Recently it has been shown that the modification of the surface layers of MSs is a process that almost does not have limitations [29]. In particular, the amphiphilic silica sol was obtained by the third method (hydrolytic polycondensation of tetraethoxysilane) (Scheme 5) by termination after condensation with alkoxysilane bearing two tails: decyl and ethylene oxide (triethylene glycol). The investigation of the resulting particles by the Langmuir method showed that the ordering of the low-molecular fraction of nanogels at the air–water interface is accompanied by the formation of aggregate structures of interpenetrating macromolecules after decomposition of the liquid-like Langmuir layer. These aggregates do not fully decompose during further compression–expansion cycles. The aggregate structures of the high-molecular fractions decompose reversibly to the primary objects during sequential compression–expansion cycles, which is characteristic of the Langmuir layers of nanoparticles. These systems hold great promise for the formation of amphiphilic layers and membranes in the ordered cell-like aggregate structures such as liposomes [30, 31] and colloidosomes [32, 33].

Summarizing the section devoted to MSs that comprise the

<i>t</i> , min	<i>T_g</i> , °C	M:T	MM (GPC)	<i>d</i> , g/cm ³	<i>σ</i> , mN/m	<i>η</i> , dL/g	<i>R</i> , nm
30	-80.84	1:1.8	<i>M_N</i> : 2272 <i>M_W</i> : 2815 <i>M_W/M_N</i> : 1.24	1.026	20.5	0.014	0.9
60	-77.29	1:2	<i>M_N</i> : 2721 <i>M_W</i> : 4231 <i>M_W/M_N</i> : 1.55	1.044	19.7	0.015	0.9
80	-75.75	1:2.2	<i>M_N</i> : 2814 <i>M_W</i> : 4762 <i>M_W/M_N</i> : 1.70	1.046	19.4	0.016	0.9
160	-51.25	1:2.6	<i>M_N</i> : 3411 <i>M_W</i> : 7023 <i>M_W/M_N</i> : 2.06	1.087	18.8	0.021	1.4
240	-30.13	1:3.1	<i>M_N</i> : 3812 <i>M_W</i> : 10121 <i>M_W/M_N</i> : 2.66	1.110	16.8	0.025	2.1
320	-6.95	1:3.4	<i>M_N</i> : 5675 <i>M_W</i> : 34927 <i>M_W/M_N</i> : 6.15	1.130	15.3	0.039	2.9
600	54.36	1:4.1	<i>M_N</i> : 20659 <i>M_W</i> : 236661 <i>M_W/M_N</i> : 11.46	1.203	–	0.090	10.6

Table 1. Properties of the PMSSO DCNGs depending on the condensation time before termination. Designations in the table: *t* condensation time; *T_g* glass-transition point; M:T ratio of M and T units calculated based on the elemental analysis data; MM (GPC) molar mass characteristics of the PMSSO DCNGs according to the GPC data; *d* density; *σ* surface tension measured by the hanging drop method (with the accuracy of ±0.2 mN/m); *η* characteristic viscosity; *R* hydrodynamic radius.

correlation between the condensation time, composition of the structure of macromolecules, molecular and optical characteristics, as well as solution characteristics.

Table 1 summarizes the results of the investigation of this representative series of samples that allows for the estimation of sequential changes in the parameters on passing from a hyperbranched structure to a nanogel. The resulting samples represent transparent liquids, which viscosities grow as the condensation time increases. Whereas the low-molecular samples are highly mobile liquids, the high-molecular samples, being at the foot of a macrogel, represent viscous low-mobile liquids and look like high-molecular PDMSs; the final sample of the series represents a powder. Figure 3 shows the photographs of the samples.

The presented data show the sequential and regular growth of the densities and refractive indices of the nanogels, which reflects an increase in the sizes of the PMSSO core. The core-shell ratio changes almost in two times. A transition from the molecular structure to the nanogel is clearly demonstrated by the changes in the values of *T_g*. While the first samples represent

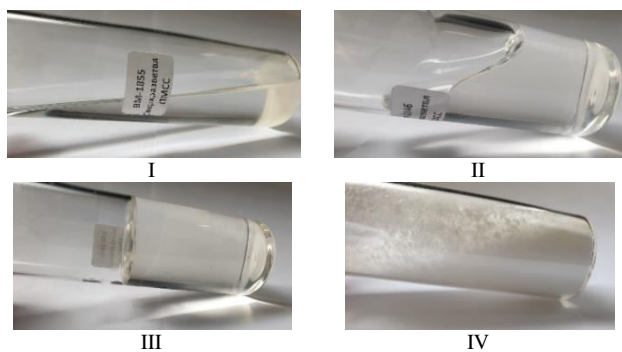


Figure 3. Photographs of the PMSSO DCNG samples: (I) 30 min (low-viscous liquid), (II) 160 min (highly viscous liquid), (III) 320 min (almost nonflowing (at room temperature) liquid), (IV) 600 min (solid powder).

mobile branched oligomers with *T_g* equal to -77 °C, an increase in the condensation time before termination leads to an increase of *T_g* to 54 °C. A difference between the fractions exceeds 130 °C. And this happens at the minimal changes in the composition formulation.

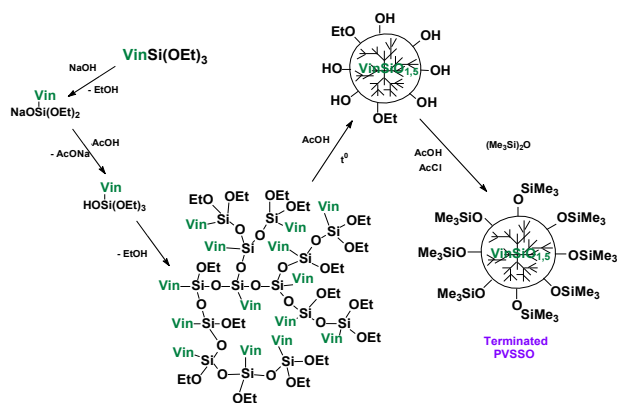
As well as in the case of the aerogels, the comparison with analogous parameters obtained for organic-inorganic systems, MSs, also shows a clear difference between the silica and PMSSO cores. The difference between the molecular and colloidal forms in the silica systems approached 400 °C, *i.e.*, more than three times higher than the analogous value for the PMSSO systems. Of note is also a smooth transition from a macromolecule to a particle in the PMSSO systems, which makes them very convenient for investigation; even the typical colloidal samples retain the mobility and represent liquids at room temperature. This offers opportunities to study the changes in their rheological parameters in the whole range of the core-shell ratios. Furthermore, the resulting dependences of the growth of refractive indices on the PMSSO composition allow for the definition of the compositions of newly synthesized PMSSOs without recourse to complex analytical methods.

Hence, the PMSSO nanogels actually comprise a new type of polymethylsiloxane liquids, which principally differ from their linear and branched analogs. Of course, they merit detailed investigation with a search for effective application fields. It is noteworthy that, analogously to the silica nanogels, the PMSSO nanogels are molecular composites by their nature since they have broad molar-mass distribution and, as it is obvious from the data of Table 1, the difference in the value of molar masses defines a complex of physicochemical characteristics. This means that, analogously to the systems with the silica cores, they contain the plasticizing fractions and the fractions that play the role of polymer matrices. Apparently, the detailed investigations of their properties, such as heat conductivity, compressibility, bulk dilatation coefficients, dielectric characteristics, can offer new application fields for them both as

individual working liquids and in compositions with conventional PMS samples.

Polymethylvinyl- and phenylsiloxane nanogels

A transition from silica cores of nanogels to PSSO cores showed that not only modification of the shell but also variation of the core can be used to control the properties of new objects and, thereby, demonstrated the possibilities of DCNGs. Thus, the displacement of the silica core for the polymethylsilsesquioxane core afforded the so-called nanoliquids, which were formed in a broad range of the core-shell ratios and molar masses [37]. In this context, an important experiment was carried out using the well-developed scheme that sequentially furnished sodium vinyl(diethoxy)silanolate, hyperbranched polyvinylsilsesquioxane, and DCNG on its base terminated with trimethylsilyl groups [38]. Scheme 8 presents the synthetic process.

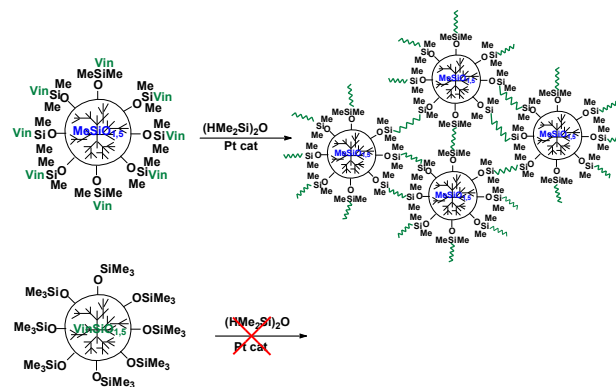


Scheme 8. Synthesis of hyperbranched polyvinylethoxysiloxanes and polyvinylsilsesquioxane nanogels.

Furthermore, using the same scheme, a mirror copy of the vinyl-containing DCNG was synthesized. Hence, two types of the copolymer samples were obtained that had identical chemical compositions but principally differed in the positions of vinyl groups (in the first case, they were located in the core, while in the second case, they were included in the shell composition). The synthesis of these objects allowed us to obtain the purely chemical proof of the core-shell structure of these hybrid macromolecules. Scheme 9 shows the results of the hydrosilylation of the DCNGs with functional groups in the molecule composition.

The vinyl groups of the external DCNG layer appeared to be rather active, which led to the rapid formation of a three-dimensional macronetwork. At the same time, their analogs covered under the inert trimethylsilyl shell did not enter the reaction and the systems remained the same—fully soluble and with the unchanged molar masses, which was confirmed by the GPC data. The trimethylsilyl coating reliably hid the sterically hindered cores of the vinylsilsesquioxane nanogel from the reagent, especially if take into account that the hydrosilylation requires certain space for an intermediate complex.

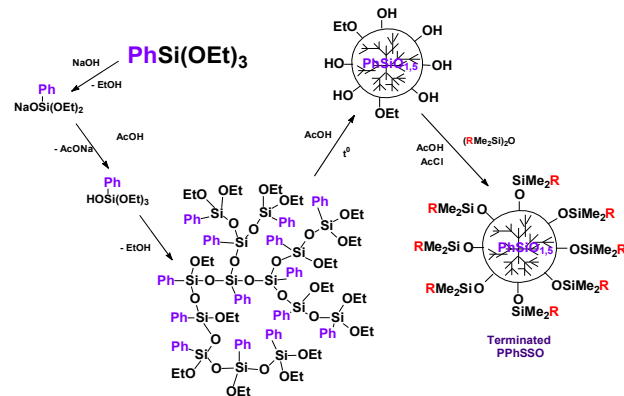
Besides purely model functions, the resulting PMSSO nanogels bearing functional groups in the shell were used in a



Scheme 9. Hydrosilylation of DCNGs with the vinyl groups in the core and shell.

range of chemical transformations which will be considered further in the section devoted to the prospects of the practical application of DCNGs with different functional groups.

Besides the nanogels with methyl and vinyl groups at the silsesquioxane silicon atoms, the same method can be used to obtain other DCNGs. In particular, phenylsilsesquioxane nanogels were reported [39, 40] that were obtained by the polycondensation in an active medium of the preliminarily synthesized hyperbranched polyphenylsilsesquioxanes. Using the scheme developed for the conversion of macromolecules to colloidal particles, a series of polyphenylsilsesquioxane nanogels were obtained at different condensation times before the addition of the terminating agent (Scheme 10). Tetramethyldivinylsiloxane was used as a terminating agent. As the condensation time in an active medium increases, the ratio of the core and shell sizes also changes. For the rheological analysis, a phenylsilsesquioxane nanogel bearing dimethylphenylsiloxy groups in the shell was also obtained. The resulting polyphenylsilsesquioxane was divided into three fractions by fractional precipitation: the fractions with the mass peaks of 1400, 2860, and 3850 a.m.u. The analysis of the flow curves at different temperatures showed that the viscosities of all the samples did not depend on the shear rate. This implies that all the samples were the Newtonian liquids. As the molar mass of a nanogel increases, the viscosity also grows; however, it should be noted that, on passing from the molar mass of 1400 to 2860 a.m.u., the viscosity grows multiply. Such a drastic change



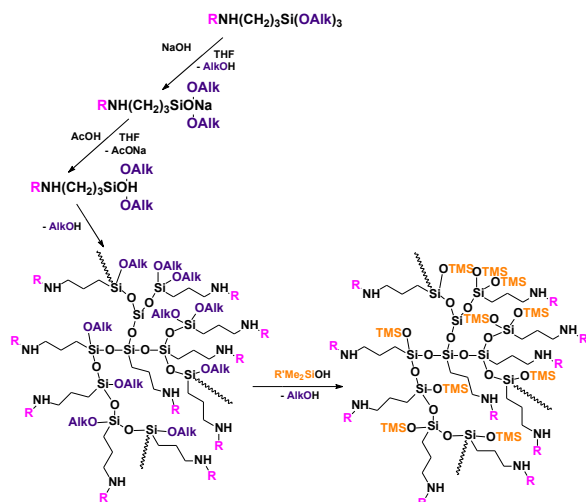
Scheme 10. Synthesis of hyperbranched polyphenylethoxysiloxanes and polyphenylsilsesquioxane nanogels (R is methyl, vinyl, phenyl, or any other organic group).

in the physical properties at the minimal changes in the chemical compositions is a characteristic feature of these objects, which clearly demonstrates the interrelation between structure and properties observed earlier for other nanogels.

The temperature dependences of the oligomer viscosities were used to calculate the viscous flow activation energy. In the case of the most low-molecular nanogel, the activation energy was not defined since the dependence was not linear. The nanogels with the higher molar masses had very high activation energies at about 190 kJ/mol. The data of TGA analysis showed that all the samples possess high thermal stabilities up to 410–450 °C.

Organofunctional hyperbranched polymers

The application of the approaches used in the synthesis of alkoxy sodium salts to amino-functionalized alkoxy silanes extended this type of monomers and enabled the synthesis of their derivatives, among which of particular importance for us are hyperbranched polymers and nanogels on their base. Scheme 11 demonstrates the synthetic routes to the salts based on amino-substituted alkoxy silanes. The synthetic method was essentially modified, the excess of alkoxy silane was excluded; it can be assumed that the amino groups significantly affected the formation of a transition complex during interaction of the alkoxy silane with sodium hydroxide [41].



Scheme 11. Synthesis of alkoxy sodium salts of aminoalkoxy silanes ($R = H, -CH_2CH_2NH_2$; $Alk = Me, Et$) and their conversion to hyperbranched polymers ($R' = Me, Vin$; $TMS =$ trimethylsilyl, or dimethylvinylsilyl terminating group).

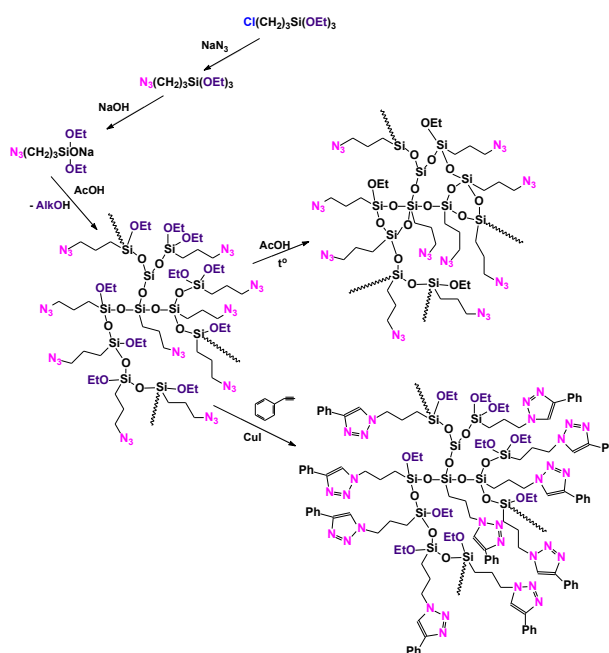
The presence of a large amount of the residual alkoxy groups in the structures of the resulting polymers enables further modification of molecular structures of the branched polymers by polymer analogous transformations that lead to the formation of polymer shells of different chemical natures. Thus, resulting aminopolyethoxysiloxane is readily terminated with silanols by the ethoxy groups due to the presence of amino groups in their composition, which catalyze the substitution of the alkoxy groups. The same scheme was used to obtain hyperbranched polyethylenediaminopropylmethoxysiloxane featuring ethylene diamine groups at the ends. The termination at the alkoxy groups was carried out using dimethylvinylsilanol or

trimethylsilanol. The polymer matrices with ethylene diaminopropyl substituent at the silicon atoms showed the propensity to stabilize silver nanoparticles, whereas the monomeric aminopropylalkoxy silanes did not exhibit the stabilizing ability under these conditions.

This suggests that the introduction of amino groups into the composition of the substituents in silsesquioxane structures significantly modified the properties of polyethoxyorganosiloxanes and their terminated derivatives. An important feature of the resulting systems is their solubility in water, which, in combination with the high coordination ability of amino groups and the demonstrated ability of these polymer systems to stabilize metallic nanoparticles, makes these compounds promising versatile polymeric matrices.

Yet another nitrogen-containing hyperbranched polysilsesquioxane was obtained recently [42] using an analogous scheme starting from azidopropyltriethoxysilane. It was shown that the formation of a cross-linked product starts in 4 h of the condensation in acetic acid. The termination of the silicon functional groups was not accomplished by the standard scheme. The hyperbranched structure was modified by click chemistry technique using phenylacetylene. This afforded quantitative conversion of the azido groups to the triazole rings, with the molecular backbone of the macromolecule remaining intact (Scheme 12). The synthesis of the new azido-containing Rebrov salt essentially extends their synthetic potential and, in particular, demonstrates the prospects of further application of three types of functional groups for the formation of a molecular backbone and its modification.

Taking into account that the conventional termination of ethoxy groups at any condensation step allows one to control the density of a polycyclic core, the nitrogen-containing modifications of the Rebrov salts and hyperbranched polymers on their base can be referred to the most versatile systems among the above-mentioned counterparts. They not only allow



Scheme 12. Synthesis of a sodium salt of azidopropyltriethoxysilane and hyperbranched silsesquioxane on its base and modification of silsesquioxanes with phenylacetylene by the azide groups.

one to accomplish the deepest structural modifications but also enable tuning of the properties of nanogels on their base over a wide range. Thus, they can be used as a basis for the synthesis of both organo- and water-soluble systems.

MQ copolymers

MQ copolymers, better known as MQ resins, amount to one of the oldest and widely used organosilicon materials. For a long time, the ratio of reagents and the limits that provide the products which do not form cross-linked macrogel structures, despite an essential excess of the average system functionality above 2, implying the gel formation at low conversions of the functional groups, were chosen empirically. It was obvious that this is connected with the high cyclization degree during polycondensation. An assumption about their structures was made almost only in 50 years of active use. Arkles [43] suggested a scheme for the structural arrangement of these polymers in the form of a silica core surrounded by a trimethylsilyl shell. Some researchers consider MQ resins as sets of individual compounds [44], which is valid, as well as for each copolymer, but testifies a total misunderstanding of the polymer nature of these systems by the authors.

Modern investigations showed that, first of all, MQ resins have nanogel structures. This follows from the dependence of their characteristic viscosities on the molecular masses and the modeling of synthesis of these systems with the separate formation of the core and only then the formation of the shell. Secondly, MQ resins are actually composite materials that consist of liquid fractions playing the plasticizing role, solid but melting fractions that play the role of a polymer matrix, and, finally, solid fractions that represent nonmelting colloidal particles and serve as a molecular filler in this polymer system. Owing to the fact that the structures of all three fractions are identical and represent nanogels with different core-shell ratios, they are compatible with each other and form a molecular composite which properties are defined by the ratio of the three mentioned fractions. The latter, in turn, is defined by the ratio of the initial reagents during synthesis [18, 21, 36, 37].

In general, DCNGs are rather popular phenomena. The analysis and comparison of the data on the primary and low-branched polysilane products allowed one to attribute them during the known polydimethylsilane–polymethylcarbosilane rearrangement to DCNG [45]. The results of the measurement of characteristic viscosities of dilute solutions of polycarbosilane in polar and nonpolar solvents are typical for globular systems. Based on the GPC data obtained using the universal calibration by polystyrene standards, it was established that the hydrodynamic radii of the globules range within 1.0–7.6 nm. The additional studies of the solutions by SAXS revealed that the maximum values of the gyration radius are within 10 nm, while the mean sizes almost correspond to the hydrodynamic radius. The correlation of these values points to the shape of the molecular globules close to the spherical one and the high density of their molecular structures. The integral curve in the Kratky coordinates confirms the size distribution of particles with the maximum at about 5 nm. According to the transmission spectroscopy data, the molecular globules with a high density are observed; the shapes of these globules are close to spherical

and their sizes range from 3 to 5 nm. Hence, the performed analysis of the peculiarities of molecular structures of ceramic-forming carbosilanes indicates the dense globular nanogel structure of their molecules. This conclusion explains the low viscosity of the melts of ceramic-forming carbosilanes and the difficult control over cross-linking (curing) of the samples during thermal processing.

It can be stated for sure that the analogous comprehensive analysis of many siloxane binding agents derived from mixtures of monomers with the functionality value $f > 2.5$ will show that, by the organization of molecular structures, they are DCNGs. Consequently, to interpret their properties and a route for further improvement, one should proceed from the new concepts about their structures instead of the use of conventional empirical approaches.

Applications of DCNGs

Our review would have been incomplete if we had not discussed the main directions of the practical application of DCNGs. As it was shown above, DCNGs are compact nanoscale formations with core-shell structures. Their dual nature of macromolecule-particles, on the one hand, allows one to consider them as promising objects for the application as fillers, and, on the other hand, enables fine-tuning of their properties, which only enhances their potential as molecular fillers. The current data on the prospects of application DCNGs include the following four main directions:

- the use of DCNGs as nanoscale molecular fillers;
- the use of DCNGs as noncrystallizing liquids with colloidal flow character;
- the use of DCNGs as curing agents;
- the use of DCNGs as matrices for stabilization of metal nanoparticles.

Let us sequentially consider these directions and evaluate their prospects and define the actions required for intensive practical application of DCNGs. For the first direction, one should start with MQ copolymers, which application is already enormous in scale but is not classified by the effect. These compounds are used as plasticizing [46] and tackiness [47] agents in the compositions sensitive to pressure and for many other assignments [48–53]. Such diversity of applications and observed effects can be explained, first of all, by their compositions [25], which we discussed above. Depending on the ratio of M and Q units, the plasticizing or strengthening effect of their application prevails. The understanding of the structural organization of these polymeric colloids allows for controlling their properties and tuning them for certain polymeric matrices. For example, it allows one to use the broadened range of ratios towards an increase in the content of Q units. In the resins with phenyl substituents, it is possible to reach the values of $Q:M > 2$. Recently, new polyimide-organosilicon compounds with MQ resins were developed as binding agents for carbon fiber composites [54]. Hybrid MQ:IDA binding agents (imide-containing oligomers with terminal anhydride and *N*-acylamine units) demonstrate higher heat resistance in the air. The thermal stability of the carbon fiber composite in the inert atmosphere is analogous to that of polyimide (PI) binding agents, while in the air it is higher than that of net PI. Hence, MQ resins improve the

resistance of PI to thermal oxidation in the air. The electron microscopy studies show that the components of MQ1:1 (1 phenyl group at the M silicon atom):IDA are well compatible (there are no clear interfaces between the components) unlike those of MQ1:2 (1 phenyl group):IDA and MQ1:2 (2 phenyl groups):IDA.

In general, whereas common methyl-substituted MQ copolymers are used very extensively, the application of phenyl-substituted analogs is only gaining popularity. Their peculiarity consists in the fact that the sizes of an inorganic core can be greater and the phenyl-containing shell provides higher compatibility with aromatic polymeric matrices.

The modification of a surface layer of the molecular structures of MQ copolymers and DCNGs based on MSs allows one to use a great diversity of modifying agents and, as a result, to obtain a great diversity of DCNGs that have enhanced affinity to one or another polymeric matrix. Continuing the version of phenyl-substituted systems, of note are the examples of two-step modification of MSs with the formation of phenylethyl surfaces in the resulting nanogels [24]. The silica modified with phenylethyl groups was combined with polystyrene *via* the introduction of a molecular filler into the polymer melt. Certain molecular parameters of the nanofiller ensured homogeneous distribution of the particles over the polymer matrix. Transparent extrudates obtained in the case of the silica with different fillers evidenced that just these molecular parameters provided the maximum affinity with the matrix. The analysis of the SAXS curves suggested the independence of the filler behavior in the matrix at different filling levels: the scattering curves are identical in the whole range of measurements. Another important result that follows from the curve analysis is the relatively low intensity of scattering in the range of small angles, which evidences the lack of particle aggregation. The main scattering comes to the objects with the characteristic sizes of 2–3 nm, which is in good agreement with the particle sizes of the filler in use. According to the results of thermophysical studies, the composites obtained had only one glass-transition point, which is the most important parameter for homogenization of the nanofiller over the polymer matrix. At 25 °C polystyrene can dissolve 20 vol % (26 wt %) of silica sol. This relatively high compatibility confirms the shielding of the core of this particle and the bonds by grafted groups.

The viscosity and glass-transition points of the systems reduce with an increase of the filler content. However, the molecular structure of the core of a hybrid nanoparticle defines both its own elastic modulus and the elastic modulus of the whole composite and also affects the rate and activation energy of segmental motion in the polymer. The results obtained suggest that, upon an increase in the filler content, the characteristics of nanocomposites based on an amorphous glassy polymer are defined by a combination of the factors such as thermodynamic compatibility of an organic layer of nanoparticles with a matrix polymer, the ratio of the sizes of the macromolecules with kinetic elements that take part in a single motion action (R_m), and the size of the core of hybrid nanodamages (R_{cor}).

The organic surface layer of the nanoparticles indeed serves as a compatibilizer for the polymer-nanoparticle system and acts as a specific solvent in the matrix polymer. When the concentration of the hybrid nanoparticles in the material

increases, the solvent content in the polymer also grows. In the description of concentration dependences of rheological and relaxation properties of these nanocomposites, it is necessary to take into account that these properties are determined by the characteristics of the nanoscale filler, dispersion medium, and the properties of the matrix polymer, which change under the action of the organic surface layer of the particles.

Serenko *et al.* [27] tried to introduce the silica sol particles with polar groups in the shell, which were obtained by the hydrosilylation of a hydride-functionalized silica sol with an allyl ether of diethylene glycol bearing a methoxy group at the end, into a poly(ethylene oxide) matrix. The following matrices were used: PEG-100, PEG-400, and PEO-100000. Based on the interference patterns of the resulting blends, it was concluded that the compatibility of the MS having the diethylene oxide groups on the particle surface with PEG is restricted and depends on the molar mass of PEG (the maximum value of 15% for PEG-100 and 5% for PEG-400). There was no compatibility between the modified particles and the PEO melt. However, extrusion blending can improve the compatibility at the filler content of up to 2% without deterioration of the matrix properties. The introduction of a greater amount of the filler leads to embrittlement. The results obtained show that the complete compatibility of DCNG with the matrix, which it was tuned for, requires a thorough selection of the modifying layer that is achieved in a range of materials, as we will see further.

An analogous approach was used in the work with another matrix [26], where a silica sol with trihydroxypropyl groups in the shell was introduced into polylactide by extrusion. The composite samples represented colorless transparent films. Their transparency testifies at the qualitative level the absence of large aggregates that can scatter the light in the visible region of the spectrum. According to the analysis of the composites by SAXS intensity, the dependence of the content of nanoscale particles on their brutto content in the polymer represents a direct line with the slope coefficient almost equal to unity. This means that all the introduced particles of the modified silica sol were dispersed in the polylactide to the nanoscale level, *i.e.*, do not form micron aggregates.

Furthermore, the above-mentioned silica sols with acetoxy and methoxyacetoxy groups in the shell were also introduced into polylactide by extrusion blending [28]. According to the results of microscopic studies, both separate inclusions and a small amount of cluster agglomerates are observed in the resulting composites. The size range of these formations is rather broad. However, it is assumed that the maximum size of the agglomerates increases with the deterioration of the compatibility of the surface groups with the matrix polymer. Consequently, in the case of the particles with hydroxypropyl surface groups, the maximum size of the agglomerates does not exceed 230 nm, for the acetoxy groups it is no more than 300 nm, and for the (methoxyacetyl)oxy groups—no more than 500 nm. It should be noted that the maximum diameters of the agglomerates strongly depend on the compatibility of the matrix and surface groups and, to a lesser extent, on the size and concentration of the particles. Therefore, if the compositions are obtained by extrusion blending, the use of hybrid particles, which organic shell is highly compatible with the matrix polymer, indeed prevents the formation of agglomerates with the diameters beyond the nanometer scale. The sizes of a small

amount of large agglomerates do not exceed 300 nm.

The analysis of the composites shows that the hybrid particles with the radii of 0.7 nm act as plasticizing agents and secondary nucleating agents for the crystallization of the matrix polymer. In the nanoparticle concentration range under consideration (up to 20 wt %), the maximum reduction in the glass-transition point reaches 12.8 °C and that for the cold crystallization temperature—up to 22 °C. The most significant changes in the specific crystallization heat of the matrix polymer composite are observed upon filling of PLA with (methoxyacetyl)oxy derivatives of MSs with a particle radius of 0.7 nm. The melting points of the composites as well as the initial points of crystallization temperatures are less sensitive characteristics of the material towards the particle content and the type of the grafted surface groups. The introduction of the particles with the radii of 1.5 or 1.7 nm into PLA does not affect the temperature of the composite glass-transition independent of their sizes, nature of the surface groups, and the level of matrix compatibility. The temperature of cold crystallization reduces by 13 °C only in the case of the (methoxyacetyl)oxy derivatives.

Hence, the nanocomposites can be obtained by extrusion blending without preliminary disaggregation of a mixture, if the hybrid particles with organic shells well compatible with the matrix polymer are used. The chemical structure of the surface layer of the nanoparticles as well as their sizes and concentration are important factors for the control of the structure and properties of a polymer nanocomposite. The changes in these parameters of the filler allow one to carry out the controlled modification of the composite characteristics, in particular, to remove one of the PLA drawbacks—the low crystallization rate.

The high solubility and functionality of DCNGs enable their *in situ* use in the production of composite materials during combined processing of DCNG and a polymer matrix. One of the first versions of this approach was studied by the introduction of a nonterminated silica sol into the crazed high-density polypropylene and polyethylene [55]. The uniaxial tension of the polymers in a solution of the sol in THF (concentration 3.5%) was studied. The application of a molecular solution of the sol in THF as an adsorption active medium almost does not affect the porosity of the polymers. However, the formation of a solid phase of silica during solvent removal has a stabilizing effect on the porous structure of crazing during annealing. The high-resolution transmission electron microscopy was used to study in detail the composite structure. It was established that the whole volume of the polymer matrices is uniformly filled with SiO₂ nanoparticles with diameters of 5–15 nm, which corresponds to the sizes of the initial particles of silica sol in the solution. Hence, the direct introduction of the silica sol solution into the polymer films using crazing afforded polymer/silica sol nanocomposites. The structures based on silica sol and methylsilsesquioxane were introduced into crazed porous matrices of high-density polyethylene [56]. Instead of the sol or methylsilsesquioxane themselves, their precursors, namely, hyperbranched polyethoxysiloxane or hyperbranched polyethoxymethylsilsesquioxane were introduced. This afforded polymer nanocomposites with uniform distribution of the modified silica forms over the whole volume of the polymer matrix, which was confirmed by the electron microscopy studies of the composites obtained.

The polyethoxysiloxane precursor found application in the production of silica sol colloidosomes and microcapsules [57, 58]. For example, Zhao *et al.* [58] suggested an approach for the microencapsulation of organic liquids in solid silica. The microcapsules were prepared using low-content Pickering emulsions and hyperbranched polyethoxysiloxane as interphase binding agents for silicon dioxide particles obtained by the Stöber method. The encapsulation efficiency of this method was very high and reached almost 100%. It was shown that the encapsulation of oils in silica colloidosomes reduces the rate of their evaporation and increases the activation energy of the evaporation process. Moreover, due to brittleness of the shell, the silica colloidosomes with encapsulated oil can be considered as promising systems with controlled release, where the compounds are released under the action of a mechanical force. This method offers new opportunities for the construction of functional inorganic microcapsules and microencapsulation of hydrophobic compounds.

MS and its hyperbranched precursor were successfully used to increase the stability of polyimide (PI) coatings to the action of atomic oxygen [59]. It was shown that the introduction of the MS particles into PI leads to a reduction in the polymer erosion under the action of atomic oxygen, *i.e.*, the PI–MS composite possesses the improved resistance to atomic oxygen. A composition of the PI–MS composite was determined that provides uniform dispersing of the silica sol particles in the polymer bulk, which explains the improved stability of the PI–MS polymer-inorganic composition to the action of atomic oxygen. Thus, the amorphous silica sols can be considered as promising modifying agents for the polymers of aerospace assignment, in particular, PI.

PI was also treated with a silica sol precursor—hyperbranched polyethoxysiloxane. The films of thermoplastic PI obtained by the thermal cyclization of polyamidoacid (PI precursor) with different concentrations of the HBPEOS particles were studied. The formation of SiO₂ particles includes several stages: the hydrolysis of HBPEOS, polycondensation that leads to coarsening of the particles, and interaction of the particles with oxygen plasma that initiates the thermooxidative destruction of organic moieties of the molecules and leads finally to the formation of SiO₂ particles. The performed investigations showed that the introduction of the silica sol molecular particles into the polymer matrix in the amount of 1–10 wt % enables a reduction in the volume and mass erosion factors of the polymer in 2–3 times. The scanning electron microscopy studies revealed the changes in the morphology of the polymer surfaces after irradiation and showed that the silica particles are uniformly dispersed in the polymer bulk, which explains the improved stability of the PI–MS polymer-inorganic composition to the action of atomic oxygen. Subsequently, these results were excelled many times upon application of branched functional metallosiloxane oligomers (BFMSO) as molecular precursors in the composition of the PI polymer matrices [60, 61]. However, it should be emphasized that the formation of nanoscale filler aggregates in the polymer matrix body occurred simultaneously with the film drying. Depending on the nature of a metal in the composition of a metallosiloxane oligomer, the sizes and shape of the resulting metallosiloxane nanoparticles drastically differed. A significant role was played by the nature of the polymer matrix. Using polyetherketones as examples, it

was demonstrated that the matrix stabilizes the particles at the early growth steps and prevents their aggregation [62–64].

The opportunities of this approach appeared to be especially noticeable upon the application of siloxane liquid rubbers as a polymer matrix. In this case, BFMSOs played the roles of both the cross-linking agent and the catalyst for hydrolysis and condensation of ethoxysilyl groups. The use of BFMSO in a combination with HBPEOS in a broad range of the ratios allowed for controlling the content of the silica phase in a wide interval. The growth and formation of the structure of silica particles, in this case, have much in common with the production of terminated silica sols. The role of the terminating agent is played by the resulting polymer network. Actually, two networks are formed: one is elastomeric, which parameters are defined by the molar mass of the liquid rubber in use (20000–100000 a.m.u.), and the second one is inorganic (Fig. 4). The nature of the metal in the BFMSO composition defines the kinetics of formation of both of them and, consequently, the degree of harmony between them. Therefore, at almost comparable ratios of the reagents, the properties of the resulting vulcanizates, transparent strong films, drastically differ from each other, depending on the metal used in the BFMSO composition [65, 66].

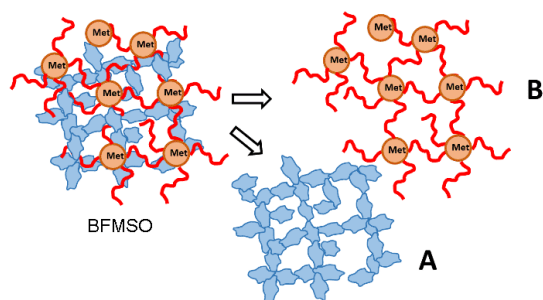


Figure 4. BFMSO structure consisting of two networks: elastomeric (A) and inorganic (B).

Hence, the versions of the so-called liquid filling, *i.e.*, the formation of a solid phase of the filler from a combined solution with a polymer matrix appeared to be an efficient method for the production of molecular composites with the use of MS and their functional precursors.

Turning to the discussion of the examples of the application of DCNGs as vulcanizing agents, one should return to the above-mentioned systems of liquid filling. At separate steps of the liquid filling, the molecular particles of silica sols are formed that can play the role of vulcanizing agents for liquid rubbers. In the original patent, this role of the HBPEOS–BFMSO mixture was mentioned specially [67]. The rest examples are connected with the functionalization of the nanogels during termination. The use of DCNG as a vulcanizing agent can be illustrated by the synthesis of phenylsilsesquioxane nanogels and their termination with the vinyl-containing alkoxy silane followed by the application of the resulting vinyl-functionalized DCNG to cure polydimethylsiloxane with hydride terminal groups by hydrosilylation. This afforded transparent uniform films [39] with the content of the polyphenylsilsesquioxane nanogel of 5, 10, 20, and 30 wt % relative to PDMS. The TGA analysis of these samples showed that all the films possess high heat resistance up to 350 °C. The amount of the coke residue

increases proportionally to the nanogel content from 23% to 60%, respectively. An increase in the nanogel content in the composition led to essential changes in the Young modulus. The tension curves show that, on passing from 5 to 30 wt % of the nanogel content, this parameter increases almost in 60 times. The strain-to-rupture reduces from 380% to 80%. As the nanogel concentration increases, it starts to fulfill also the role of the filler in the compositions, besides the role of the cross-linking agent.

The less expected application field of DCNGs appeared to be the stabilization of metal nanoparticles. The high concentration of functional groups, which can be concentrated both on the periphery and in the core of DCNGs, offers opportunities for the stabilization of different metal-containing objects under homogeneous conditions. The application of an active shell can be exemplified by the PMSSO nanogel bearing vinyl groups in the shell. Using it, the systems of superparamagnetic particles of Fe stabilized in the nanogel matrix were obtained by the ligand exchange method [68]. It was established that the nanogels stabilize the metal particles with sizes within 2–3 nm. Subsequently, the Fe/PMSSO system was used as an efficient modifier for the formation of metal-containing hybrid materials based on ultrahigh-molecular-weight polyethylene. The modification of Fe nanoparticles with the organosilicon polymer leads to the formation of a nanocomposite that contains the particles with the FeO–Fe₂O₃ core-shell structure. According to the authors, the formation of the nanocomposite occurs in two steps. The first one proceeds *in situ* via the interaction of bis(toluene)iron with the polymer, resulting in the intermediate. The second stage of the formation of a metallic nanostructure occurs in the air during the preparation of a hybrid material with the nanogel.

The use of a macromolecule core to stabilize silver nanoparticles was illustrated by hyperbranched 1,2,3-triazoloragnoethoxysiloxane [42]. The ultras-small silver nanoparticles with the average sizes < 10 nm obtained during radiation reduction in the presence of the above-mentioned polymer can be of particular interest for the development of catalytically active materials. The periphery of the resulting hyperbranched polymers, which consists of the remaining ethoxy groups, can be readily modified through the termination reactions, which afford a new type of the highly functionalized core-shell derivatives with the topological structures appropriate for a range of high-tech applications, such as nonlinear optics, drug delivery systems, and so on.

Conclusions

Hence, DCHGs are at an ascending branch of their development both from the viewpoint of further expansion of a product range and a search for effective practical applications of these objects. A unique combination of dual molecular-colloidal nature, diversity of synthetic routes, and almost unlimited opportunities for structural modifications, variety of functional precursors and routes for their conversion to DCHGs—all this offers ample opportunities for the real relevance and perspective of this field both in the nearest future and in the long term.

An important feature of this type of macromolecular objects is the fact that their diversity will be expanded not only owing to

the synthesis of new structures, which were multiply illustrated in this review, but also owing to the understanding of a nanogel nature of the existing systems, as it was demonstrated with MQ copolymers and polycarbosilane precursors of ceramics.

Acknowledgements

This work was supported by the Russian Foundation for Basic Research, project nos. 18-29-25053 and 18-29-17049.

The authors are grateful to the full member of the Russian Academy of Sciences A. M. Muzafarov for fruitful discussion and useful remarks.

Corresponding author

* E-mail: ivanbm@ispm.ru. Tel: +7(495)332-5853 (I. B. Meshkov)

References and notes

§ For Russian readers this is a customary phrase which is not controversial; let us remember, for instance, the Old New Year which is celebrated in Russia annually.

1. A. V. Kabanov, S. V. Vinogradov, *Angew. Chem., Int. Ed.*, **2009**, *48*, 5418–5429. DOI: 10.1002/anie.200900441
2. S. V. Vinogradov, T. K. Bronich, A. V. Kabanov, *Adv. Drug Delivery Rev.*, **2002**, *54*, 135–147. DOI: 10.1016/S0169-409X(01)00245-9
3. J. K. Oh, R. Drumright, D. J. Siegwart, K. Matyjaszewski, *Prog. Polym. Sci.*, **2008**, *33*, 448–477. DOI: 10.1016/j.progpolymsci.2008.01.002
4. L. Zha, B. Banik, F. Alexis, *Soft Matter*, **2011**, *7*, 5908–5916. DOI: 10.1039/C0SM01307B
5. J.-H. Ryu, R. T. Chacko, S. Jiwanpanich, S. Bickerton, R. P. Babu, S. Thayumanavan, *J. Am. Chem. Soc.*, **2010**, *132*, 17227–17235. DOI: 10.1021/ja1069932
6. Y. Jiang, J. Chen, C. Deng, E. J. Suuronen, Z. Zhong, *Biomaterials*, **2014**, *35*, 4969–4985. DOI: 10.1016/j.biomaterials.2014.03.001
7. P. J. Flory, *Principles of Polymer Chemistry*, Cornell Univ. Press, Ithaca, New York, **1953**.
8. A. M. Muzafarov, N. G. Vasilenko, E. A. Tatarinova, G. M. Ignat'eva, V. M. Myakushev, M. A. Obrezkova, I. B. Meshkov, N. V. Voronina, O. V. Novozhilov, *Polym. Sci., Ser. C*, **2011**, *53*, 48–60. DOI: 10.1134/S1811238211070022
9. A. M. Muzafarov, A. V. Bystrova, N. G. Vasilenko, G. M. Ignat'eva, *Russ. Chem. Rev.*, **2013**, *82*, 635–647. DOI: 10.1070/RC2013v082n07ABEH004406
10. A. M. Muzafarov, E. A. Tatarinova, N. G. Vasilenko, G. M. Ignat'eva, in: *Organosilicon Compounds: Experiment (Physico-Chemical Studies) and Applications*, V. Ya. Lee (Ed.), Acad. Press, **2017**, vol. 2, ch. 8, 323–382. DOI: 10.1016/B978-0-12-814213-4.00008-3
11. P. R. Dvornic, D. A. Tomalia, *Curr. Opin. Colloid Interface Sci.*, **1996**, *1*, 221–235. DOI: 10.1016/S1359-0294(96)80008-2
12. V. V. Kazakova, V. D. Myakushev, T. V. Strelkova, N. G. Gvazava, A. M. Muzafarov, *Dokl. Chem.*, **1996**, *349*, 190–193.
13. V. V. Kazakova, V. D. Myakushev, T. V. Strelkova, A. M. Muzafarov, *Polym. Sci., Ser. A*, **1999**, *41*, 283–290.
14. E. A. Rebrov, A. M. Muzafarov, *Heteroat. Chem.*, **2006**, *17*, 514–541. DOI: 10.1002/hc.20280
15. X. Zhu, M. Jaumann, K. Peter, M. Möller, C. Melian, A. Adams-Buda, D. E. Demco, B. Blümich, *Macromolecules*, **2006**, *39*, 1701–1708. DOI: 10.1021/ma052179+
16. V. V. Kazakova, E. A. Rebrov, V. D. Myakushev, T. V. Strelkova, A. N. Ozerin, L. A. Ozerina, T. B. Chenskaya, S. S. Sheiko, E. Yu. Sharipov, A. M. Muzafarov, *ACS Symp. Ser.*, **2000**, *729*, 503–515. DOI: 10.1021/bk-2000-0729.ch034
17. RU Patent 2039765 C1, **1991**.
18. N. V. Voronina, I. B. Meshkov, V. D. Myakushev, T. V. Laptinskaya, V. S. Papkov, M. I. Buzin, M. N. Il'ina, A. N. Ozerin, A. M. Muzafarov, *J. Polym. Sci., Part A: Polym. Chem.*, **2010**, *48*, 4310–4322. DOI: 10.1002/pola.24219
19. E. V. Egorova, N. G. Vasilenko, N. V. Demchenko, E. A. Tatarinova, A. M. Muzafarov, *Dokl. Chem.*, **2009**, *424*, 15–18. DOI: 10.1134/S0012500809010042
20. E. A. Tatarinova, E. A. Rebrov, V. D. Myakushev, I. B. Meshkov, N. V. Demchenko, A. V. Bystrova, O. V. Lebedeva, A. M. Muzafarov, *Russ. Chem. Bull.*, **2004**, *53*, 2591–2600. DOI: 10.1007/s11172-005-0159-x
21. E. Tatarinova, N. Vasilenko, A. Muzafarov, *Molecules*, **2017**, *22*, 1768. DOI: 10.3390/molecules22101768
22. N. V. Voronina, I. B. Meshkov, V. D. Myakushev, N. V. Demchenko, T. V. Laptinskaya, A. M. Muzafarov, *Nanotechnol. Russ.*, **2008**, *3*, 321–329. DOI: 10.1134/S1995078008050078
23. I. B. Meshkov, V. V. Kazakova, O. B. Gorbatshevich, N. V. Voronina, V. D. Myakouchev, A. M. Muzafarov, *Polym. Prepr. (Am. Chem. Soc., Div. Polym. Chem.)*, **2006**, *47*, 1152–1154.
24. A. V. Bystrova, N. V. Voronina, N. V. Gaevoy, E. V. Getmanova, O. B. Gorbatshevich, E. V. Egorova, I. B. Meshkov, A. N. Ozerin, E. A. Tatarinova, A. M. Muzafarov, *Nanotechnol. Russ.*, **2008**, *3*, 46–50.
25. V. V. Kazakova, A. S. Zhiltsov, O. B. Gorbatshevich, I. B. Meshkov, M. V. Pletneva, N. V. Demchenko, G. V. Cherkayev, A. M. Muzafarov, *J. Inorg. Organomet. Polym. Mater.*, **2012**, *22*, 564–576. DOI: 10.1007/s10904-011-9605-4
26. A. S. Zhiltsov, I. B. Meshkov, T. S. Kurkin, O. B. Gorbatshevich, V. V. Kazakova, A. A. Askadskii, O. A. Serenko, A. N. Ozerin, A. M. Muzafarov, *Nanotechnol. Russ.*, **2013**, *8*, 644–654. DOI: 10.1134/S1995078013050157
27. O. A. Serenko, V. G. Shevchenko, A. S. Zhiltsov, V. E. Chuprakov, T. V. Zaderenko, O. T. Gritsenko, M. V. Mironova, O. B. Gorbatshevich, V. V. Kazakova, V. G. Kulichikhin, A. M. Muzafarov, *Nanotechnol. Russ.*, **2013**, *8*, 81–91. DOI: 10.1134/S1995078013010138
28. A. Zhiltsov, O. Gritsenko, V. Kazakova, O. Gorbatshevich, N. Bessonova, A. Askadskii, O. Serenko, A. Muzafarov, *J. Appl. Polym. Sci.*, **2015**, *132*, 41894. DOI: 10.1002/app.41894
29. V. V. Kazakova, O. B. Gorbatshevich, Yu. N. Malakhova, A. I. Buzin, A. M. Muzafarov, *Russ. Chem. Bull.*, **2018**, *67*, 2088–2097. DOI: 10.1007/s11172-018-2333-y
30. C. Has, P. Sunthar, *J. Liposome Res.*, **2019**, *30*, 336–365. DOI: 10.1080/08982104.2019.1668010
31. A. Yaroslavov, A. Efimova, N. Smirnova, D. Erzunov, N. Lukashev, I. Grozdova, N. Melik-Nubarov, *Colloids Surf., B*, **2020**, *190*, 110906. DOI: 10.1016/j.colsurfb.2020.110906
32. C. Zhang, C. Hu, Y. Zhao, M. Möller, K. Yan, X. Zhu, *Langmuir*, **2013**, *29*, 15457–15462. DOI: 10.1021/la404087w
33. H. Jiang, Y. Sheng, T. Ngai, *Curr. Opin. Colloid Interface Sci.*, **2020**, *49*, 1–15. DOI: 10.1016/j.cocis.2020.04.010
34. K. Kanamori, K. Nakanishi, *Chem. Soc. Rev.*, **2011**, *40*, 754–770. DOI: 10.1039/C0CS00068J
35. A. M. Muzafarov, in: *Efficient Methods for Preparing Silicon Compounds*, H. W. Roesky (Ed.), Acad. Press, **2016**, 179–181. DOI: 10.1016/B978-0-12-803530-6.00013-5
36. A. I. Amirova, O. V. Golub, I. B. Meshkov, D. A. Migulin, A. M. Muzafarov, A. P. Filippov, *Int. J. Polym. Anal. Charact.*, **2015**, *20*, 268–276. DOI: 10.1080/1023666X.2015.1013185
37. A. Ya. Malkin, M. Yu. Polyakova, A. V. Subbotin, I. B. Meshkov, A. V. Bystrova, V. G. Kulichikhin, A. M. Muzafarov, *J. Mol. Liq.*, **2019**, *286*, 110852. DOI: 10.1016/j.molliq.2019.04.129

38. D. Migulin, E. Tatarinova, I. Meshkov, G. Cherkaev, N. Vasilenko, M. Buzin, A. Muzafarov, *Polym Int.*, **2016**, *65*, 72–83. DOI: 10.1002/pi.5029
39. M. N. Temnikov, *PhD Dissertation*, Moscow, **2017**.
40. M. N. Temnikov, M. I. Buzin, N. V. Demchenko, G. V. Cherkaev, N. G. Vasilenko, A. M. Muzafarov, *Mendeleev Commun.*, **2016**, *26*, 121–123. DOI: 10.1016/j.mencom.2016.03.012
41. D. Migulin, S. Milenin, G. Cherkaev, E. Svidchenko, N. Surin, A. Muzafarov, *J. Organomet. Chem.*, **2018**, *859*, 24–32. DOI: 10.1016/j.jorganchem.2017.11.028
42. D. Migulin, S. Milenin, G. Cherkaev, A. Zezin, E. Zezina, A. Muzafarov, *React. Funct. Polym.*, **2020**, *154*, 104648. DOI: 10.1016/j.reactfunctpolym.2020.104648
43. B. Arkles, *MRS Bull.*, **2001**, *26*, 402–408. DOI: 10.1557/mrs2001.94
44. D. H. Flagg, T. J. McCarth, *Macromolecules*, **2016**, *49*, 8581–8592. DOI: 10.1021/acs.macromol.6b01852
45. P. A. Storozhenko, G. I. Shcherbakova, A. M. Muzafarov, A. N. Ozerin, N. V. Voronina, M. Yu. Mitrofanov, D. V. Sidorov, D. V. Zhigalov, M. Kh. Blokhin, E. M. Gizullina, M. G. Kuznetsova, M. V. Polyakova, G. Yu. Yyrki, *Nanotekhnika*, **2009**, *4*, 7–12.
46. M. Di, S. He, R. Li, D. Yang, *Nucl. Instrum. Methods Phys. Res., Sect. B*, **2006**, *248*, 31–36. DOI: 10.1016/j.nimb.2006.02.017
47. N. Amouroux, J. Petit, L. Leger, *Langmuir*, **2001**, *17*, 6510–6517. DOI: 10.1021/la010146r
48. H. Xiang, J. Ge, S. Cheng, H. Han, S. Cui, *J. Sol-Gel Sci. Technol.*, **2011**, *59*, 635. DOI: 10.1007/s10971-011-2538-0
49. X. Shi, Z. Chen, Y. Yang, *Eur. Polym. J.*, **2014**, *50*, 243–248. DOI: 10.1016/j.eurpolymj.2013.11.005
50. P. Jia, H. Liu, Q. Liu, X. Cai, *Polym. Degrad. Stab.*, **2016**, *134*, 144–150. DOI: 10.1016/j.polymdegradstab.2016.09.029
51. M. V. Mironova, I. B. Meshkov, A. A. Shabeko, V. V. Shutov, V. G. Kulichikhin, E. A. Tatarinova, *INEOS OPEN*, **2020**, *3*, 29–34. DOI: 10.32931/io2004a
52. N. V. Sergienko, T. V. Strelkova, K. L. Boldyrev, L. I. Makarova, A. S. Tereshchenko, *INEOS OPEN*, **2019**, *2*, 196–199. DOI: 10.32931/io1928a
53. Q. Wang, W. Li, L. Zhang, J. Zhang, W. Xiong, Y. Wu, B. Song, Y. Mai, *Polym. Sci., Ser. B*, **2020**, *62*, 306–318. DOI: 10.1134/S1560090420030173
54. E. N. Popova, V. E. Yudin, L. A. Myagkova, V. M. Svetlichnyi, E. A. Tatarinova, A. M. Muzafarov, N. N. Saprykina, V. Yu. Elokhovskii, G. V. Vaganov, *Russ. J. Appl. Chem.*, **2013**, *86*, 1873–1879. DOI: 10.1134/S1070427213120124
55. E. S. Trofimchuk, N. I. Nikonorova, E. A. Nesterova, A. M. Muzafarov, I. B. Meshkov, A. L. Volynskii, N. F. Bakeev, *Nanotechnol. Russ.*, **2009**, *4*, 736. DOI: 10.1134/S199507800909016X
56. N. I. Nikonorova, E. S. Trofimchuk, I. B. Meshkov, A. L. Volynskii, N. F. Bakeev, A. M. Muzafarov, *Nanotechnol. Russ.*, **2015**, *10*, 888–895. DOI: 10.1134/S1995078015060087
57. H. Wang, X. Zhu, L. Tsarkova, A. Pich, M. Möller, *ACS Nano*, **2011**, *5*, 3937–3942. DOI: 10.1021/nn200436s
58. Y. Zhao, Y. Li, D. E. Demco, X. Zhu, M. Möller, *Langmuir*, **2014**, *30*, 4253–4261. DOI: 10.1021/la500311y
59. K. B. Vernigorov, A. Yu. Alent'ev, I. B. Meshkov, A. M. Muzafarov, E. N. Voronina, L. S. Novikov, V. N. Chernik, *Inorg. Mater.: Appl. Res.*, **2012**, *3*, 81–87. DOI: 10.1134/S2075113312020177
60. U. Andropova, O. Serenko, N. Tebeneva, A. Tarasenkov, M. Buzin, E. Afanasyev, A. Polezhaev, A. Naumkin, L. Novikov, V. Chernik, E. Voronina, A. Muzafarov, *Polym. Test.*, **2020**, *84*, 106404. DOI: 10.1016/j.polymertesting.2020.106404
61. O. A. Serenko, U. S. Andropova, D. A. Sapozhnikov, M. I. Buzin, N. A. Tebeneva, V. N. Chernik, L. S. Novikov, E. N. Voronina, A. V. Kononenko, *J. Surf. Invest.: X-Ray, Synchrotron Neutron Tech.*, **2018**, *14*, 275–280. DOI: 10.1134/S1027451020020330
62. U. S. Andropova, M. S. Parshina, N. A. Tebenev, A. N. Tarasenkov, M. I. Buzin, V. V. Shaposhnikova, O. A. Serenko, A. M. Muzafarov, *Russ. Chem. Bull.*, **2018**, *67*, 230–237. DOI: 10.1007/s11172-018-2063-1
63. U. S. Andropova, N. A. Tebeneva, O. A. Serenko, A. N. Tarasenkov, M. I. Buzin, V. V. Shaposhnikova, A. M. Muzafarov, *Mater. Des.*, **2018**, *160*, 1052–1058. DOI: 10.1016/j.matdes.2018.10.033
64. U. S. Andropova, N. A. Tebeneva, A. N. Tarasenkov, M. S. Parshina, A. A. Askadskii, O. A. Serenko, A. M. Muzafarov, *Polym. Sci., Ser. B*, **2017**, *59*, 202–209. DOI: 10.1134/S1560090417020026
65. N. A. Tebeneva, I. B. Meshkov, A. N. Tarasenkov, N. V. Polshchikova, A. A. Kalinina, M. I. Buzin, O. A. Serenko, Y. V. Zubavichus, D. E. Katsoulis, A. M. Muzafarov, *J. Organomet. Chem.*, **2018**, *868*, 112–121. DOI: 10.1016/j.jorganchem.2018.04.011
66. A. N. Tarasenkov, N. A. Tebeneva, M. S. Parshina, I. B. Meshkov, N. G. Vasilenko, G. V. Cherkaev, G. P. Goncharuk, D. E. Katsoulis, A. M. Muzafarov, *J. Organomet. Chem.*, **2020**, *906*, 121034. DOI: 10.1016/j.jorganchem.2019.121034
67. RU Patent 2014114570, **2014**.
68. A. Yu. Vasil'kov, D. A. Migulin, A. V. Naumkin, O. A. Belyakova, Y. V. Zubavichus, S. S. Abramchuk, Y. V. Maksimov, S. V. Novichikhin, A. M. Muzafarov, *Mendeleev Commun.*, **2016**, *26*, 187–190. DOI: 10.1016/j.mencom.2016.04.002